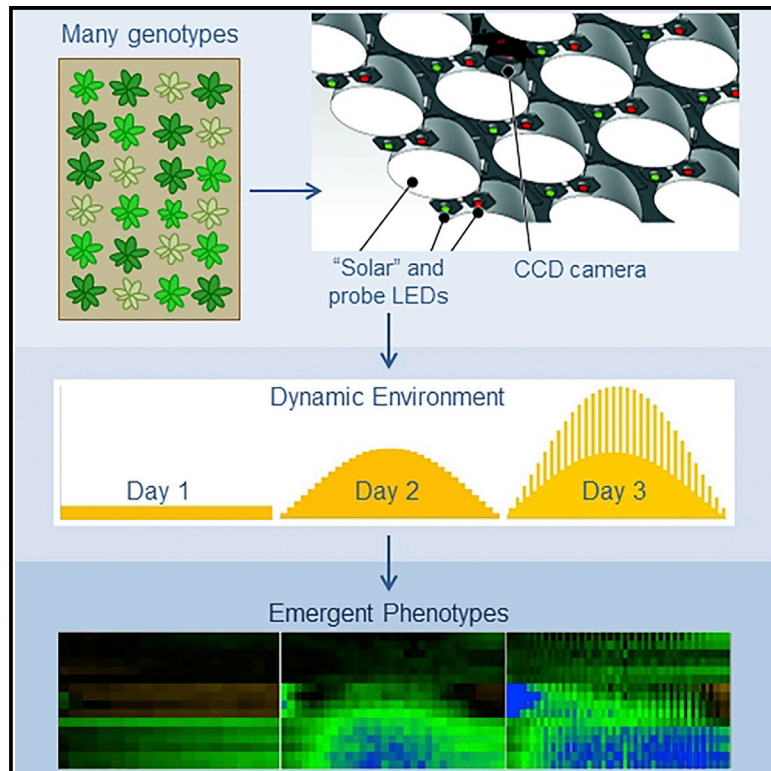# Dynamic Environmental Photosynthetic Imaging Reveals Emergent Phenotypes

Graphical Abstract

Authors

Jeffrey A. Cruz, Linda J. Savage, Robert Zegarac, ..., William Kent Kovac, Jin Chen, David M. Kramer

Correspondence

kramerd8@msu.edu

In Brief

Cruz et al. demonstrate a new, high-throughput phenotyping platform that systematically reveals the mechanisms and genetic bases of photosynthetic responses that appear under dynamic or fluctuating environmental conditions.

Highlights

- DEPI is a novel high-throughput platform for plant phenotyping

- DEPI can reveal new transient or environment-specific phenotypes

- DEPI replicates natural, dynamic, or fluctuating environmental conditions

- The platform revealed a new response of photosynthesis to fluctuating light

CellPress

Dynamic Environmental Photosynthetic Imaging Reveals Emergent Phenotypes

Jeffrey A. Cruz,[1,2] Linda J. Savage,[1] Robert Zegarac,[1] Christopher C. Hall,[1,3] Mio Satoh-Cruz,[1] Geoffry A. Davis,[1,4] William Kent Kovac,[1,3] Jin Chen,[1,5] and David M. Kramer[1,2,3,*]
[1]MSU-DOE Plant Research Laboratory
[2]Biochemistry and Molecular Biology
[3]Plant Biology
[4]Cell and Molecular Biology
[5]Computer Science and Engineering
Michigan State University, East Lansing, MI 48824, USA
*Correspondence: kramerd8@msu.edu
http://dx.doi.org/10.1016/j.cels.2016.06.001

SUMMARY

Understanding and improving the productivity and robustness of plant photosynthesis requires high-throughput phenotyping under environmental conditions that are relevant to the field. Here we demonstrate the dynamic environmental photosynthesis imager (DEPI), an experimental platform for integrated, continuous, and high-throughput measurements of photosynthetic parameters during plant growth under reproducible yet dynamic environmental conditions. Using parallel imagers obviates the need to move plants or sensors, reducing artifacts and allowing simultaneous measurement on large numbers of plants. As a result, DEPI can reveal phenotypes that are not evident under standard laboratory conditions but emerge under progressively more dynamic illumination. We show examples in mutants of *Arabidopsis* of such "emergent phenotypes" that are highly transient and heterogeneous, appearing in different leaves under different conditions and depending in complex ways on both environmental conditions and plant developmental age. These emergent phenotypes appear to be caused by a range of phenomena, suggesting that such previously unseen processes are critical for plant responses to dynamic environments.

INTRODUCTION

Plants live in highly dynamic and unpredictable environments, requiring phenotypic flexibility that is particularly important in photosynthesis for maintaining tradeoffs among the efficiency of light energy capture, resource requirements and availabilities, and the avoidance of deleterious side reactions. This flexibility is especially important under high and fluctuating light intensities when the rate of light capture exceeds photosynthetic capacity, leading to the production of reactive oxygen species (ROS). Hence, the photosynthetic machinery is delicately balanced to

provide the right amount of energy, at the right times, in the correct forms without damaging or killing the organism (Raven, 2011; Murchie and Niyogi, 2011; Kramer and Evans, 2011). This integrated regulation is particularly important under fluctuating environmental conditions (Kramer and Evans, 2011; Suorsa et al., 2012) and involves a wide range of regulatory phenomena, including modulation of biophysical properties of light-capturing machinery, allosteric regulation of enzymes, post-translational modification of proteins, and gene regulation, leading to changes in enzyme levels or morphological properties (Kramer and Evans, 2011; Tikkanen et al., 2012; Rascher and Nedbal, 2006).

Improving photosynthetic energy capture for increased food and fuel production will require readjustments in this fine balancing because regulatory processes that prevent photodamage also tend to reduce the efficiency of energy capture; e.g., by increasing the dissipation of light energy in the antenna complexes (Blankenship et al., 2011; Zhu et al., 2010). At the same time, it is imperative that, under all conditions, productive yield be maximized to offset losses caused by environmental perturbations (Boyer, 1982; Vadez et al., 2012). Thus, engineering or selecting for useful adjustments in photosynthetic performance will require an understanding of the roles and mechanisms of the critical regulatory components of photosynthesis.

Plant photosynthesis research has largely been conducted under artificially static conditions in controlled environment chambers. These "standard laboratory conditions" provide reproducible experimental designs and have greatly advanced our understanding of the biochemical, structural, biophysical, and physiological bases of the core processes involved in photosynthesis. However, these approaches can miss important components that are required for robust and efficient photosynthesis in the rich, dynamic environments encountered in the field. In support of this view, recent studies have shown that mutations that disrupt known photosynthetic regulatory processes can have small effects on growth and/or photosynthetic performance under unchanging laboratory conditions but produce strong phenotypes under rapid fluctuations in environmental conditions (Kramer and Evans, 2011; Tikkanen et al., 2012; Gaspar et al., 2002). For example, the *npq4* mutant lacks photoprotective energy-dependent exciting quenching (q_E) or the rapid response component of non-photochemical quenching (NPQ),

but higher levels of photodamage and corresponding decreases in "fitness" are only seen when grown under fluctuating light or natural environments (Külheim et al., 2002). Similarly, a state transition mutant (*stn7*) and a proton gradient regulation mutant (*pgr5*) do not accumulate photosystem I (PSI) damage until shifted to growth under fluctuating light (Grieco et al., 2012; Suorsa et al., 2012). In addition, environmental growth conditions clearly influence the development of photosynthetic capacity over longer timescales (Mishra et al., 2012; Grieco et al., 2012). Collectively, these observations confirm that both long- and short-term effects of the growth environment must be considered.

It is now recognized that detailed phenotyping under appropriate conditions, an approach we term "environmental phenometrics," is critical for understanding and improving plant yield (Munns et al., 2010). Photosynthetic productivity and robustness are determined by highly complex sets of traits and depend on many interacting factors related to both maximizing efficiency (Zhu et al., 2010; Blankenship et al., 2011) and coping with environmental stress (Boyer, 1982; Vadez et al., 2012). Thus, environmental phenometrics requires non-invasive probes of relevant phenotypes that can be applied to many plants over an extensive range of conditions and multiple time frames.

There is a vast amount of literature regarding the application of in vivo spectroscopic techniques to plants. Well established methods include gas exchange (Long and Bernacchi, 2003), chlorophyll *a* fluorescence spectroscopy (Baker and Oxborough, 2004), kinetic absorbance and reflectance spectroscopy (Baker et al., 2007; Kramer and Crofts, 1996), 3D plant imaging (Omasa et al., 2007; Paproki et al., 2012), thermal imaging (Sirault et al., 2009; Munns et al., 2010), and hyperspectral radiometry (Stroppiana et al., 2009). Each of these techniques has provided useful new information, but generally at discrete time points and/or on individual plants or leaves, and there are several major challenges to applying these techniques for phenotype-driven plant screening, selection, and engineering for improved photosynthesis. For example, to achieve high throughput, these techniques must be automated but cannot disturb the physiological status of the plants. Some current approaches rely on mechanized transport of plants to sensors or sensors to plants, e.g., the "conveyor" system, typified by the TraitMill (GB, CropDesign), the PlantScreen (Photon Systems Instruments), and Scanalyzer (Lemnatec) systems. In the conveyer systems, numerous plants can be grown in special pots on a network of automated conveyor belts that move the plants to enclosed chambers for measurements. This approach has already been used for assessing plant architecture, overall biomass, chlorophyll content, drought responses, and nitrogen assimilation (Roy et al., 2011). Although valuable, there are several limitations for the conveyor approach, particularly when attempting to assess the effects of environmental fluctuations. Funneling the plants into a limited number of chambers requires that plants be measured at different times of the day, obscuring shorter-term variations induced by diurnal cycles or environmental fluctuations. Enclosing plants in measuring chambers can perturb light capture, metabolism, and gene expression and mask the effects of applied environmental parameters by altering light intensity and quality throughout the canopy (Morgan and Smith, 1981), activate touch responses (Braam and Davis,

1990; Braam, 2005), induce rapid temperature fluctuations (Singsaas and Sharkey, 1998), and alter local CO_2 concentrations (Schäufele et al., 2011). Also, the need to move plants on the conveyor can severely limit the dimensions of the pots, potentially affecting root growth, nutrient uptake, and drought responses (Poorter et al., 2012). An alternative approach, developed by several groups, moves cameras and/or sensors above the plants, in chambers or greenhouses (Nedbal and Whitmarsh, 2004; Oxborough, 2004a, 2004b) or in the field (White et al., 2012), via a system of cranes, vehicles, or cables. The mobile sensor approach avoids the requirement for moving the plants and, in principle, allows more natural soil/root environments. However, the sensors can only monitor a limited number of plants/plots at a time, preventing assessment of rapid, transient, or diurnal effects. In addition, these systems require the use of non-growth wavelengths of illumination, potentially perturbing photosynthesis.

The dynamic environmental photosynthesis imager (DEPI) addresses critical limitations in previous technology and enables direct assessment of rapid and long-term responses to dynamic environmental conditions of large numbers of plants in parallel. Although expandable to many parameters, in this work we focus on DEPI measurements of photosynthesis, reflecting photosystem II (PSII) quantum efficiency (ϕ_{II}), light-driven linear electron flow (LEF), dissipative NPQ of absorbed light energy, activation of the photoprotective mechanisms through the q_E response, and onset of photoinhibition or chloroplast movements by the slow relaxation of NPQ; i.e., the q_I response. Importantly, our approach allows these measurements to be made while maintaining plants under the white (or arbitrary spectral output) LED illumination and environmental conditions that can simulate fluctuations that occur in a natural environment. In this way, DEPI can capture both short- and long-term (developmental) responses to dynamic environmental conditions.

RESULTS

High-Sensitivity Photosynthetic Imaging under Dynamic Light Conditions

DEPI is an experimental platform that integrates multiple components (imaging cameras, a high-precision lighting system, and a controlled growth environment; i.e., plant growth chamber) to allow continuous monitoring of growth and photosynthetic performance under dynamic environmental conditions. The DEPI lighting system uses an array of high-intensity white LEDs with optics that collimate the output light, thus achieving steady-state light intensities in excess of full sunlight (>2,500 μmol photons $m^{-2} s^{-1}$) at a distance of up to 1 m from the lighting array (Figure 1A; Experimental Procedures). The lights can also deliver a brief period (0.5 s to a few seconds) of saturating intensity (up to and exceeding 15,000 μmol photons $m^{-2} s^{-1}$) for measuring various chlorophyll fluorescence parameters. Fluorescence excitation light is supplied by an array of monochromatic LEDs. In the current configuration, these probe LEDs are red, but other wavelengths may also be used. Fluorescence images for all plants under the lighting array were captured simultaneously by five charge-coupled device (CCD) cameras fitted with glass filters that block visible wavelengths and pass chlorophyll fluorescence in the near-infrared.
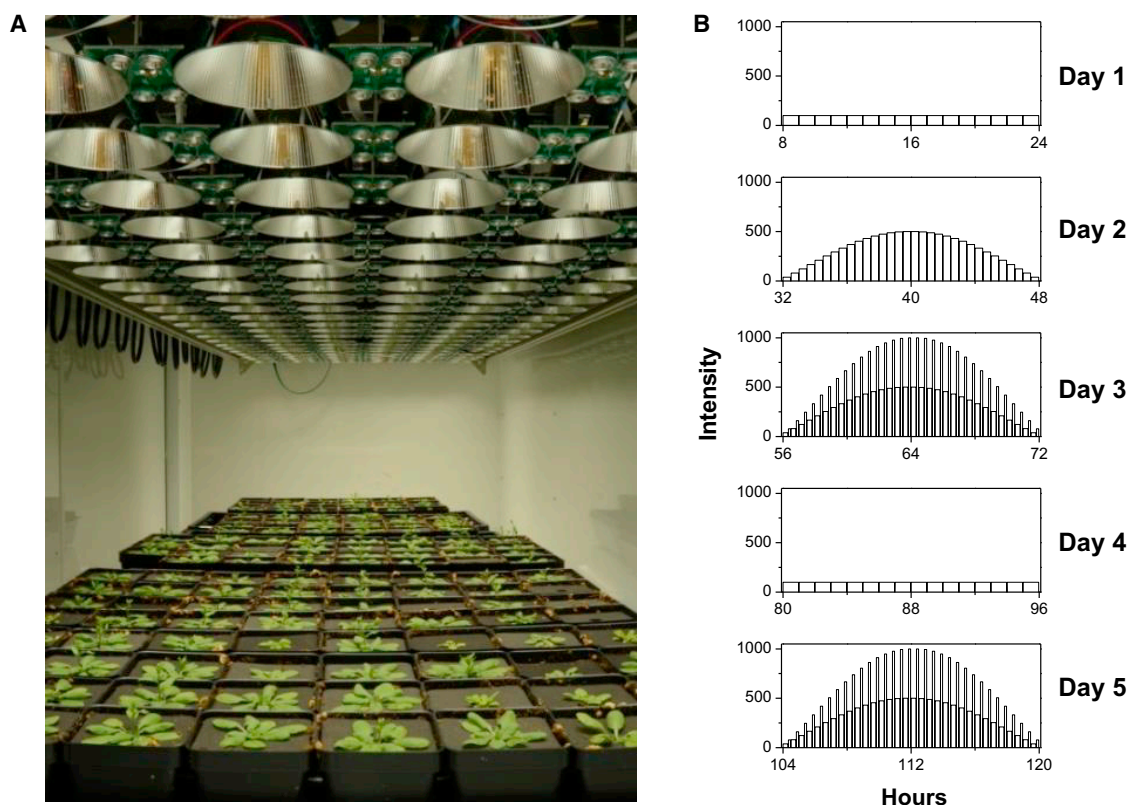
Figure 1. Tracking Photosynthetic Performance Using DEPI under REPs
(A and B) Plants were grown, and photosynthetic performance was monitored in a DEPI chamber (A) over 5 days of light intensity ramped environmental perturbations (B) sequentially going through a flat day (day 1), a sinusoidal day (day 2), a fluctuating day (day 3), a flat day (day 4), and finally a fluctuating day (day 5). A period of complete darkness was required to estimate the q_E and q_I parameters. To avoid perturbations, the frequency of these measurements (at the end of every hour on flat days or the end of each intensity change on sinusoidal and fluctuating days) and the duration of the dark period (2 min) were kept to a minimum.

To demonstrate the utility of DEPI, we measured photosynthetic parameters in a set of wild-type and mutant *Arabidopsis* plants over a 5-day period. The library of plants included wild-type Columbia-0 (Col-0) and a series of over 300 mutants lines with transfer DNA (T-DNA) insertions in chloroplast-targeted nuclear genes provided by the Chloroplast 2010 project (http://www.plastid.msu.edu/) (Lu et al., 2011; Ajjawi et al., 2010). The population of plants was grown under standard growth chamber conditions for 3 weeks and transferred to DEPI. Over the course of the experiment, we applied "ramped environmental perturbation" (REP) conditions designed to reveal phenotypes that are not typically apparent under laboratory conditions but appear under more natural fluctuating conditions (Figure 1B). On day 1, plants were exposed to a "flat" illumination day with constant, 100 μmol photons m^{-2} s^{-1} illumination for 16 hr, similar to that used in typical laboratory growth chamber experiments. Next, plants were exposed to "sinusoidal" illumination (day 2), mimicking the kinetics and intensity of solar irradiation changes over a day in the field. In this case, the maximal intensity at simulated noon was 500 μmol photons m^{-2} s^{-1}. On day 3, plants were exposed to "fluctuating" light with changes to impose the kinds of light dynamics resulting from occlusion or reflection of sunlight by clouds or leaf movements induced by wind. Specifically, the sinusoidal illumination used on day 2 was punctuated

every 30 min with 8-min fluctuation periods of doubled illumination intensity so that the peak intensity under fluctuating light was 1000 μmol photons m^{-2} s^{-1}. On day 4, plants were given 1 day to recover under flat day illumination (as on day 1), and then, on day 5, were exposed again to fluctuating light to test for acclimation responses to the initial fluctuating conditions. Because the illumination treatments were performed in sequence, the effects are likely to reflect both immediate and cumulative effects of individual conditions.

Several chlorophyll fluorescence-derived photosynthetic parameters were imaged periodically over the course of the experiment, including the quantum efficiency of PSII photochemistry ϕ_{II}, LEF, NPQ, as well as the rapidly relaxing (q_E) and slowly relaxing (q_I) components of NPQ. The q_E component reflects the activation of photoprotective energy-dependent exciton quenching, whereas the slowly relaxing component includes contributions from exciton quenching from photoinhibition or the xanthophyll cycle, state transitions, and chloroplast movements (Cazzaniga et al., 2013; Horton and Hague, 1988; Nilkens et al., 2010; Dutta et al., 2015). DEPI incorporates several technical advances that allow measurements of these chlorophyll fluorescence yields under white actinic illumination (Experimental Procedures), but the procedures for deriving the photosynthetic parameters were essentially as described previously
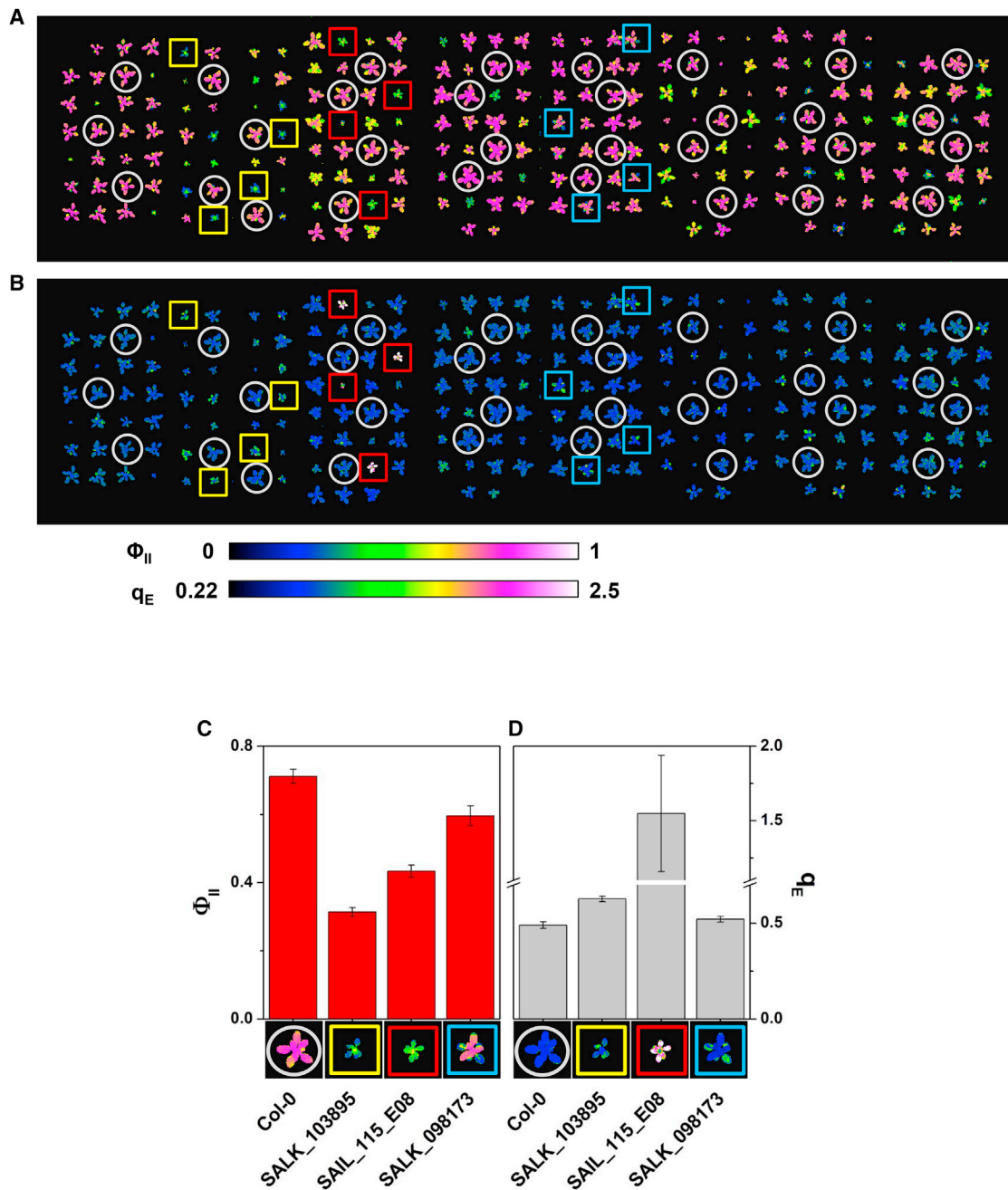
Φ_{II} 0 [color bar] 1

q_E 0.22 [color bar] 2.5

Figure 2. High-Throughput Measurements of Photosynthetic Parameters Using DEPI

(A and B) Composite images of Φ_{II} (A) and q_E (B) stitched from five camera views for 231 plants encompassing 52 mutant lines, with wild-type controls captured at the beginning of day 3 (first actinic period at an intensity of 40 μmol photons m^{-2} sec^{-1}). Each genotype is indicated by the surrounding color-coded symbols (see also labels in Figure 2C). Enclosed in squares are plants for the mutant lines SALK_103895 (NFU domain protein 3, At4g25910, yellow), SAIL_115_E08 (NADPH-dependent thioredoxin reductase, At2g41680, red), and SALK_098173 (PSB33, At1g71500, blue), and enclosed in circles are wild-types (col-0), referred to in the Results as SALK_103895, SAIL_115_E08, and SALK_098173, respectively.

(C and D) Averaged Φ_{II} (C, red) and q_E (D, gray) values are shown in bar graphs (n = 4) with representative images from (A) and (B) displayed below each bar.

(Baker and Oxborough, 2004). Under appropriate conditions, it is possible to infer from these measurements the fate of absorbed light, the activation of photoprotection, and the onset of photoinhibition and repair processes, which are critical for understanding the efficiency and environmental responses of photo-

synthesis (Baker et al., 2001). Kinetically resolved data for representative plants are described below and in Figures S1–S5. Figure 2 shows DEPI "snapshot" images of two photosynthetic parameters, ϕ_{II} (Figure 2A) and q_E (Figure 2B), captured simultaneously for 231 individual plants (representing 52 mutant

lines) at the onset of rapid fluctuations in actinic intensity that occurred after 18 min of illumination on day 3. At this time point, several mutant lines, including SALK_098173, SAIL_115_E08, and SALK_103895, showed distinct red and blue false coloring, representing high and low values for photosynthetic parameters.

To assess the reproducibility of DEPI measurements, we compared the responses of replicates across the chamber. A statistical analysis of integrated values over a full-day experiment shows that DEPI can distinguish changes in ϕ_{II} values with SDs of 2%–3% of average values (e.g., for ϕ_{II} and q_E [Figures 2C and 2D]), across individual cameras or the entire DEPI chamber. This high level of reproducibility was maintained over a period of days and was afforded by careful control of environmental and measurement parameters, especially by the use of calibrated computer control of individual banks of actinic LEDs (Experimental Procedures).

We observed that mutation-induced changes in ϕ_{II} and q_E often occur in highly spatially heterogeneous patterns (Figures 2C and 2D). For example, SAIL_115_E08 and SALK_103895 showed preferential loss of ϕ_{II} and increase in NPQ in the older (outermost) leaves, possibly reflecting the accumulation of photoinhibition or developmental differences in the structural properties or photosynthetic enzyme activities of the leaves (Baker et al., 2001). The appearance of strong heterogeneity shows that, in these (and similar) cases, it is often not possible to extrapolate photosynthetic performance from data taken only at specific locations (as is typical for spectroscopic approaches) without routine application of imaging techniques (see also a review in Nedbal and Whitmarsh, 2004). Likewise, averaging data of the entire plant will often miss important heterogeneous responses.

Effects of Changing Illumination Conditions on Photosynthesis Averaged over the Entire Plant

Of the over 300 mutant lines that were screened, we highlight the photosynthetic behavior of SALK_098173 as a prime example of an "emergent" phenotype observed under a progressively dynamic environment. We first consider simplified DEPI measurements of photosynthetic phenotypes averaged over entire plants. Figure 2 shows representative datasets from Col-0 and SALK_098173, which harbors a T-DNA insert in AT1G71500 (TAIR, www.arabidopsis.org), coding for a putative Rieske iron-sulfur domain-containing protein targeted to the thylakoid membrane (Peltier et al., 2004; Friso et al., 2004). Recently this protein has been proposed to be a component of photosystem II and designated PSB33, responsible for maintaining and stabilizing the supercomplex organization of PSII and light-harvesting complexes (Fristedt et al., 2015).

During continuous or flat illumination on day 1, Col-0 showed nearly constant photosynthetic parameters, indicating that the system was able to maintain steady-state photosynthesis over the entire day. Under sinusoidal illumination on day 2, as irradiance increased, ϕ_{II} decreased so that LEF saturated (Figure 3). Both the half-saturation point (about 160 μmol photons m^{-2} s^{-1}) and the maximal LEF (about 84 μmol electrons m^{-2} s^{-1} at mid-day) were similar to those observed in short-term exposure to saturating light in plants grown under similar conditions (Takizawa et al., 2007), suggesting that the photosynthetic capacity was not diminished by exposure to

the sinusoidal light. NPQ and its component parameters q_E and q_I increased with increasing illumination before mid-day and recovered as illumination decreased in the evening (Figure 3), predominantly reflecting the onset of and recovery from photoinhibition (Müller et al., 2001; Baker et al., 2007). Notably, the q_E parameter increased sigmoidally after a distinct lag period, probably reflecting the non-linear relationship between q_E and the acidification of the thylakoid lumen pH (Takizawa et al., 2007). On the other hand, the q_I component increased almost immediately during sinusoidal illumination, likely reflecting the activation of chloroplast movements, which contribute to the slowly recovering fluorescence signal NPQ (Cazzaniga et al., 2013; Dutta et al., 2015). The F_V/F_M parameter (dashed lines, Figure 3), a measure of the maximal quantum efficiency of PSII before illumination in the morning, was measured to be 0.82, consistent with an essentially complete recovery from any photoinhibition that occurred under laboratory chamber illumination.

On day 3, Col-0 photosynthetic parameters were strongly dependent on the fluctuating illumination conditions. During the stronger illumination periods, ϕ_{II} was suppressed whereas NPQ increased, mainly caused by upregulation of q_E. These effects largely recovered during the weaker illumination later in the day, except for a small residual suppression of ϕ_{II} at the end of the day (Figure 3), suggesting a partial loss of photosynthetic capacity. On day 4 (flat light) and day 5 (repeat of the fluctuating light day), the photosynthetic parameters for wild-type plants were nearly indistinguishable from those on days 1 and 3 (Figure 3; Figures S1 and S2), with only small changes in F_V/F_M, ϕ_{II}, and NPQ. Thus, we can conclude that, despite the fact that the plants were grown under laboratory lighting conditions, the wild-type photosynthetic system was largely able to cope with the abrupt perturbations in light intensity on days 2 and 3.

On days 1 and 2, the photosynthetic parameters for SALK_098173 were nearly identical to those in Col-0 (Figure 3). Substantial phenotypic differences only appeared on day 3 (Figure S3), with the appearance of decreased maximal PSII quantum efficiency (F_V/F_M), indicating a loss of PSII activity; decreased steady-state quantum yield (ϕ_{II}), especially early in the day; decreased q_E responses during high (and fluctuating) light, indicating a loss of photoprotective responses; and increased, slowly reversible NPQ response (q_I) increased in the mutant, especially later in the day, suggesting the accumulation of photoinhibition.

Differences in photosynthesis between SALK_098173 and Col-0 persisted into day 4 (Figure 3), with the mutant showing decreases in maximal PSII quantum yield ($F_V/F_M \sim 0.7$), possibly reflecting accumulation of photoinhibition (but see below), and decreased ϕ_{II} and LEF, particularly in the early morning, possibly reflecting limitations at the photosystems or downstream metabolic processes. The relative loss of maximal quantum efficiency in the mutant had largely recovered on the morning of day 5, but application of fluctuating light during day 5 revealed new effects of SALK_098173, most notably a suppression of the q_E response and progressive loss of ϕ_{II} and LEF (Figure S3).

Spatial and Temporal Heterogeneity of Dynamic Photosynthetic Responses in SALK_098173

Closer examination of the DEPI images revealed that SALK_098173 showed strongly heterogeneous photosynthetic
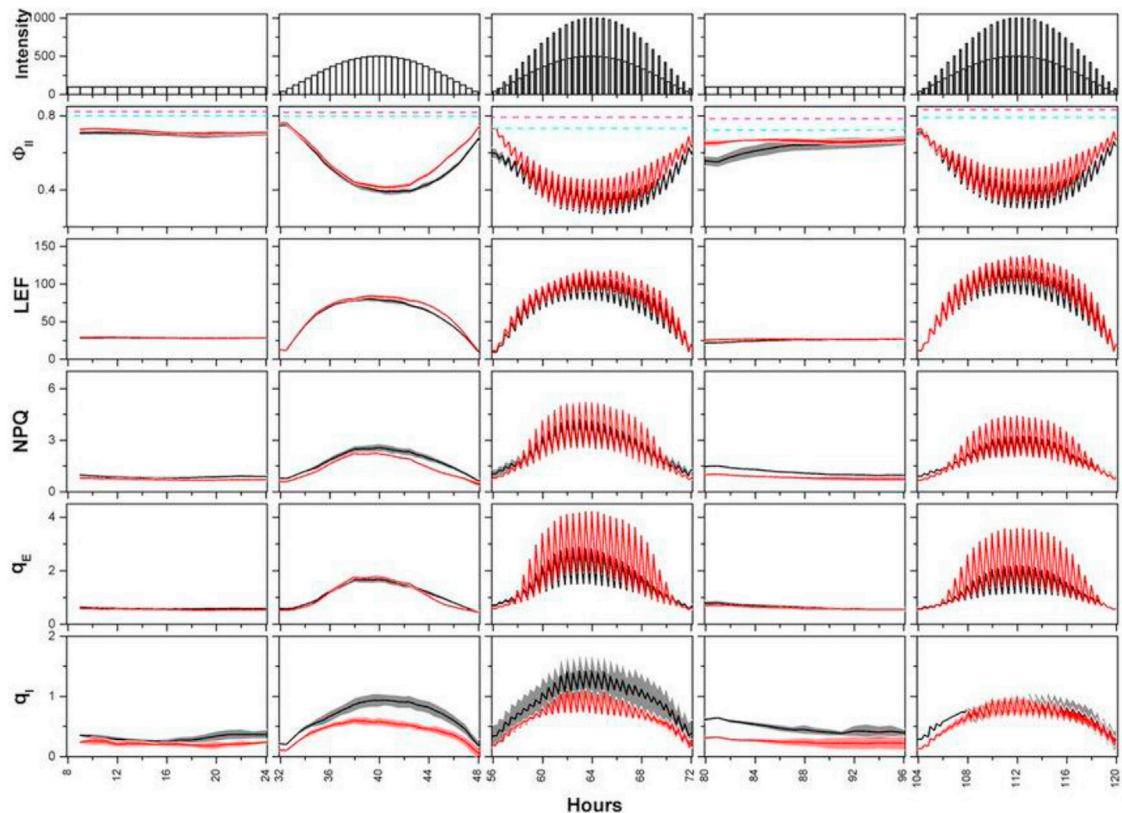
Figure 3. Emergent Phenotypes in SALK_098173
Daily light intensity changes occurring over a 5-day period are shown with corresponding averaged (n = 4) photosynthetic parameters (Φ_{II}, LEF, NPQ, q_E, and q_I) for the wild-type (Col-0, red) and SALK_098173 (SALK_098173, black), with SDs represented by the shaded areas. Dashed magenta (Col-0) and cyan (SALK_098173) lines in the plots of Φ_{II} indicate averaged F_V/F_M values. For clarity, expanded views of days 3 and 5 are presented in Figure S3.

phenotypes that depended both on leaf development and light treatment. These heterogeneous responses can be seen in the false-color images taken at selected time points (Figure 4; Figure S4; Movie S1), kinetically resolved plots of individual photosynthetic parameters (Figure S4), and in heat maps comparing parameters to the surface-averaged results from Col-0 (Figure 4B). Tissue-dependent differences were also seen in Col-0 but were much more subtle (Figure S5; Movie S2). For the purpose of this discussion, the leaves are numbered in pairs according to their developmental ages; i.e., pair 1 for the cotyledon leaves, 2 for the first rosette leaves, 3 for the next oldest rosette leaves, and so on.

Photosynthetic parameters in leaf pair 4 remained nearly indistinguishable in Col-0 and SALK_098173 over the course of the experiment, except for a somewhat elevated q_E response in the mutant during fluctuating light on days 3 and 5. In contrast, the older leaves showed strong phenotypes that appeared at unexpected times after exposure to dynamic light conditions. On day 1, under flat lighting, all leaves on the mutant and Col-0 showed similar, homogeneous photosynthetic behaviors (Figure 4B; Figures S4 and S5). Likewise, on day 2, only subtle and spatially homogeneous effects appeared in the mutant toward the end of the day, reflected in weak elevation of NPQ, q_E, and q_I (by about 10%). Strong, heterogeneous effects appeared abruptly in the mutant on the morning of day 3,

specifically in leaf pair 2 (Figure 4), with strong suppression of ϕ_{II} and elevation of NPQ. It should be noted that, to prevent disturbances, we did not assay fluorescence parameters during the night, but there were no signs of altered photosynthesis at the end of day 2, indicating that the effects appeared sometime after exposure. The phenotype was also heterogeneous within each affected leaf, affecting preferentially the outer edges and toward the apexes of the affected leaves (Figure 4; Movie S1). As a result, the false-color images showed distinct "patches," suggesting that the phenotype was caused by developmental, metabolic, or physiological factors that varied across the leaf tissue.

The ϕ_{II} parameter in the mutant gradually recovered throughout the day and became nearly indistinguishable from Col-0 throughout the rest of the experiment. The day 3 NPQ phenotype in the affected areas was attributable to effects on both q_E and q_I, with the former being especially affected at lower light in the morning and evening. The increased NPQ in the mutant decreased over days 4 and 5, although it did not fully recover, suggesting that the plant was able to partially acclimate in response to the conditions on day 3.

Very similar transient and heterogeneous phenotypes for ϕ_{II} and NPQ were seen on leaf pair 3 but were shifted later in time by about 24 hr. This general pattern was observed in multiple plants (Figure S6), suggesting that the phenotype was triggered
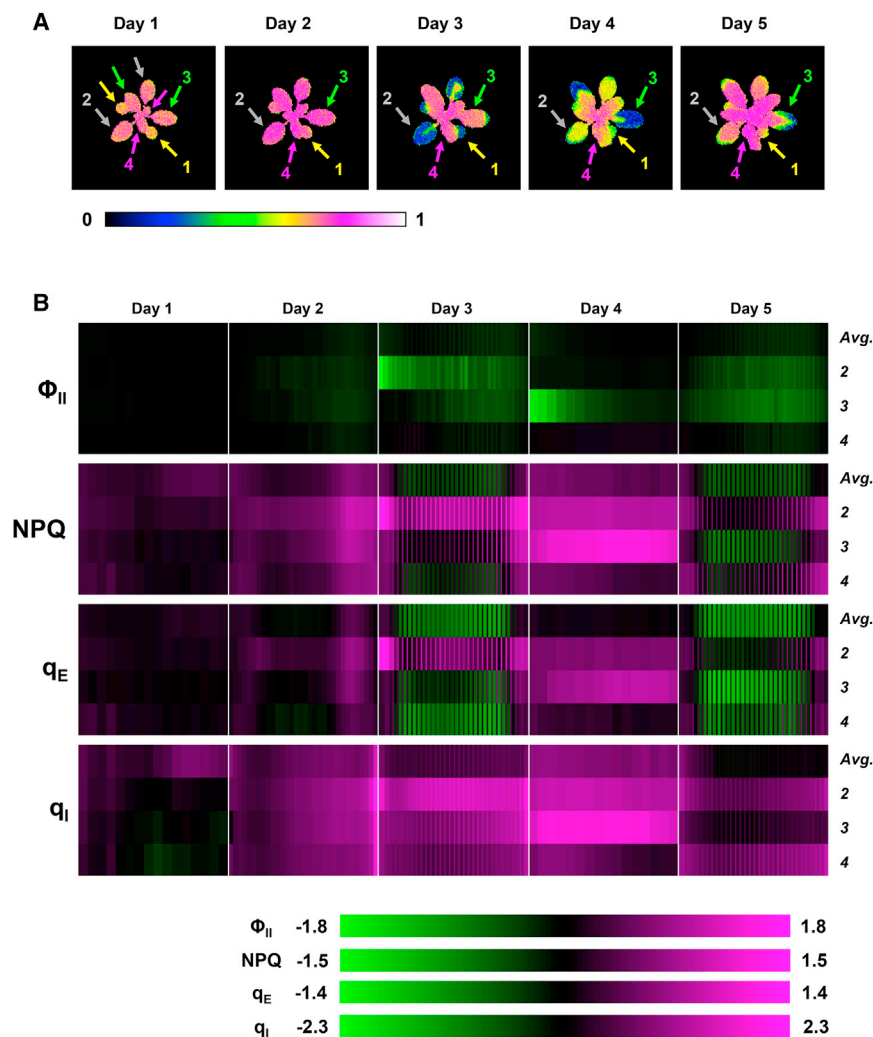
Figure 4. Spatial and Temporal Heterogeneity of Photosynthetic Performance in SALK_098173.

(A) False-color images of Φ_{II} collected early in the day are shown for a SALK_098173 plant, with arrows pointing toward specific leaf pairs as described in Results: cotyledons (yellow, leaf 1), first rosette leaves (gray, leaf 2), second rosette leaves (green, leaf 3), and third rosette leaves (magenta, leaf 4).

(B) Heat maps showing fold changes over Col-0 in the averaged photosynthetic parameters (Φ_{II}, NPQ, q_E, and q_I) of SALK_098173 (Avg.) from Figure 3B, with heatmaps for parameters obtained by sampling leaves 2, 3, and 4. Green and magenta indicate values lower and greater than the surface-averaged Col-0, respectively.

representative subset of which was already presented in Figure 2. To select mutants in an unbiased way, we developed and applied an image analysis algorithm (Experimental Procedures) that automatically scans DEPI image data and detects heterogeneous photosynthetic phenotypes based on the variance of ϕ_{II}. The *psb33-1* (SALK_098173) lines plants described above were readily detected, demonstrating the ability of the system to detect the general phenomenon. In addition, we found a number of lines with photosynthetic behaviors similar to *psb33* and describe 12 of these with the strongest phenotypes here (Figure S7). Most of these lines showed only weak phenotypes on the flat illumination on day 1 but distinct heterogeneous phenotypes on days 2, 3, or 4 (Table S1). The mutations associated with these phenotypes affect genes encoding proteins with a range of predicted functions (Table S1), including PSII stability and antenna state transitions (PsbR), photoprotection (NPQ7), triose-phosphate transport (TPT), and putative transcription factors involved in abiotic stress signaling (e.g., AT3G10470) as well as several genes of unknown functions (At1g16880, At3g46610, At5g59250, At5g08540, and At2g29180). Loci for which multiple independent knockout alleles were available showed similar phenotypes, suggesting that knocking out each of these genes independently was able to induce the phenomenon. Thus, the diversity of the genes involved implies that the phenomenon reflects the effects of multiple interacting processes.

We next sought to apply DEPI to develop and test possible mechanisms underlying the patchy phenotype. In all cases, the patchy areas showed decreased ϕ_{II} and increased NPQ (both q_E and q_I components) (data for a subset are shown in Figure 5 and Figure S7). However, there was a general trend in which decreased ϕ_{II} and increased q_E appeared very early in the day, whereas q_I tended to accumulate over time (Figures S8 and S9; Movie S3), suggesting that the mutations initially suppressed photosynthesis by feedback regulation involving the buildup of

by a combination of environmental factors (in this case, high/fluctuating light) and the developmental state of the leaf tissues.

The increased q_I and decreased ϕ_{II} in the affected areas are consistent with the previous suggestion that loss of AT1G71500 decreases the stability of PSII (Fristedt et al., 2015). However, the heterogeneous effects preceded the application of fluctuating light on day 3, implying that they were not directly caused by loss of PSII activity (photoinhibition) incurred during the previous day's exposure to sinusoidal illumination. Indeed, in leaf pair 2, photosynthetic capacity largely recovered over a few hours of illumination on day 3 despite being exposed to fluctuating illumination, which appears inconsistent with a simple role in maintaining PSII integrity. Our results instead suggest that AT1G71500 may control a nocturnally specific process critical for acclimation, remodeling, or repair of the photosynthetic apparatus in response to photoinhibition (see also below).

Insights into Development-Specific Acclimation of Photosynthesis to Light Stress

To gain further insights into the nature of the emergent "patchy" phenotypes, we further examined the fluorescence imaging data of the more than 300 T-DNA lines from the REP screening, a
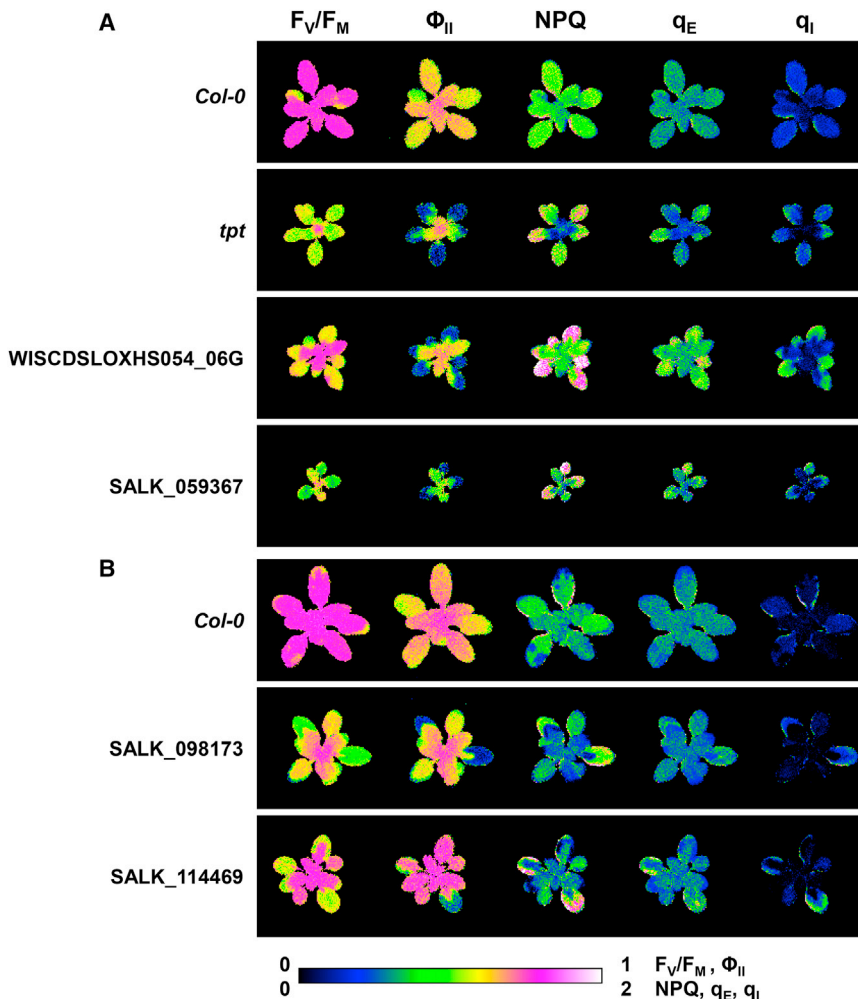
Figure 5. Identification of Other Mutants with Patchy Phenotypes

(A and B) False-color images of F_V/F_M and Φ_{II}, NPQ, q_E, and q_I after (A) ∼2 hr of actinic illumination on day 3 for *Col-0*, *tpt*, WISCDSLOXHS054_06G (ACT domain-containing protein), and SALK_059367 (pentatricopeptide repeat superfamily protein) and (B) ∼1 hr of illumination on day 4 for *Col-0*, SALK_098173 (*psb33-1*), and SALK_114469 (*PsbR*).

flashes spaced 70 ms apart (giving an average light intensity of about 10 μmol photons m^{-2} s^{-1}). In the wild-type and in non-patchy regions of the mutants, only very small changes in fluorescence yield were seen, indicating that Q_A was fully re-oxidized between flashes. However, in the patchy regions of the mutants, the fluorescence yield increased monotonically with each successive flash, indicating the accumulation of reduced Q_A^-. Because the maximal quantum efficiency for PSII photochemistry in the regions was similar to or less than that of the wild-types, this accumulation must have been caused by inhibition of Q_A re-oxidation (rather than an increase in the rate of PSII excitation). The effect was not reversed by application of far red illumination (Figure S12), which preferentially excites PSI photochemistry and thus oxidizes plastoquinol, arguing against the possibility that it was caused by reduction of the PQ pool through cyclic electron flow (CEF) or chlororespiration (Strand et al., 2015). We thus propose that the high fluorescence level at low light most likely reflects the accumulation of a substantial fraction of PSII centers in non-functional states, perhaps related to the reported upshift in Q_A redox potential that accompanies loss of Ca^{2+} from the oxygen-evolving complex (Krieger and Rutherford, 1997) or the occurrence of so-called centers inactive in electron transfer from Q_A to Q_B (Chylla et al., 1987; Chylla and Whitmarsh, 1989).

Regardless of the mechanisms, the appearance of the modified PSII behavior centers did not immediately follow exposure to high light at the end of the previous day (Movie S1; Figure 4), implying that the effect cannot be attributed to the immediate effects of photodamage. Instead, the observation that the effects are transitory and precede decreases in sensitivity of photosynthesis to subsequent exposure to fluctuating light suggests that they reflect the process of "remodeling" the photosynthetic apparatus to acclimate to fluctuating light.

DISCUSSION

By addressing limitations in current technology, the DEPI platform enables direct assessment of rapid and long-term responses of photosynthesis for a large number of plants

thylakoid *pmf* but that q_E was unable to fully protect the photosynthetic apparatus, leading to photoinhibition.

One possible mechanism for the observed effects on photosynthesis is decreased stomatal conductance, which will decrease internal CO_2 levels and thus lead to slow ATP synthase and increased *pmf* and q_E responses (Kohzuma et al., 2012; Kanazawa and Kramer, 2002). Indeed, stomatal closure has been previously associated with heterogeneous (or patchy) photosynthetic patterns (Lawson et al., 1998; Loreto and Sharkey, 1990; Mott and Buckley, 1998; Attaran et al., 2014; Bresson et al., 2015). We therefore tested whether the phenotypes we observed could be reversed under elevated CO_2, which bypasses restrictions to photosynthesis caused by low stomatal conductance. We observed varied responses to elevated CO_2 (Figures S10 and S11; Movie S4), but none of the lines showed strong suppression of patchy phenotypes, implying that the patchy phenotypes were not caused by altered stomata responses.

A subset of the patchy mutants (SALK_098173, WISCDSLOXHS054_06G, *tpt*, SALK_114469, SALK_059367) showed high fluorescence yield in their patchy regions even at very low light intensities. This effect is illustrated for selected mutants for which the effect was strongest (Figure 6), where we illuminated with a series of weakly actinic measuring
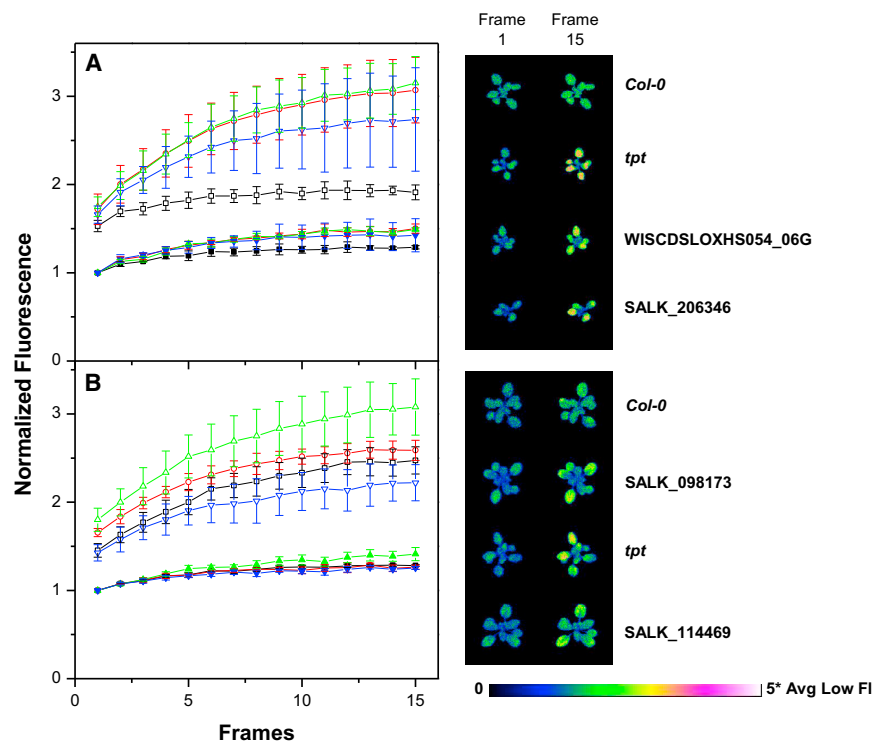
Figure 6. Heterophenotypic Regions Show Altered PSII Activity

(A) Fluorescence values for the high F_0 (open symbols) and low F_0 (closed symbols) regions of individual plants on day 3 for *Col-0* (black, n = 3), *tpt* (red, n = 5), WISCDSLOXHS054_06G (green, n = 5), and SALK_206346 (blue, n = 5) from 15 sequential frames, each given a partially actinic measuring flash.

(B) Fluorescence values for *Col-0* (black, n = 5), SALK_098173 (red, n = 4), *tpt* (green, n = 4), and SALK_114469 (blue, n = 5) on day 4. Images were collected every 70 ms, allowing Q_A^- in active PSII centers to be reoxidized. Individual traces for each line were normalized to the values of the first measuring pulse, estimated to be near the fully dark-adapted value, F_0.

To the right of each panel are representative false-color images of dark-adapted (F_0, frame 1) and the weak light-induced fluorescence yield (frame 15) for *Col-0*, *tpt*, WISCDSLOXHS054_06G from (A) and *Col-0*, SALK_098173, *tpt*, and SALK_114469 from (B) (top to bottom).

under diverse but reproducible dynamic environmental conditions. It was designed to control key environmental parameters, including temperature (4°C–44°C), humidity (25%–75% relative humidity), and illumination with white (growth) light at intensities and dynamics found in natural environments (0–2500 μmol photons m^{-2} s^{-1}). By capturing images from multiple devices and in parallel, DEPI allows sensitive imaging of chlorophyll fluorescence parameters without moving plants or cameras and with reasonable time resolution. For example, during the fluctuating day, 129 image sets were captured by five CCD cameras in a 16-hr period to generate 64 images each of ϕ_{II}, NPQ, q_E, and q_I for ~231 individual plants. In principle, it should be possible to replay arbitrary or certain field conditions (e.g., over a growing season) using the DEPI platform and capture photosynthetic and growth responses.

However, DEPI is not designed to perfectly replicate all aspects of natural environments; e.g., it cannot replicate changes in wind patterns or biotic processes such as insect attacks. Instead, the intent is to impose progressively more realistic dynamics of the environments to understand their importance for plant responses. The initial device, described here, controls the parameters most likely to have an immediate effect on photosynthesis (especially light fluctuations, temperature, and humidity) while providing an extendable platform for incorporation of new technologies that can better mimic natural environments. However, we note that, even with these parameters, there exist certain limitations. For example, the white LED illumination in the current version of the instrument does not perfectly replicate the solar spectrum (Shur and Zukauskas, 2005) or changes in light quality that occur over the course of the day. In particular, the current LEDs have relatively low fluence in UV (<425 nm) and far red (700–740 nm) components and excess fluence in

the blue (440–460 nm) wavelength ranges, known to excite photoreceptors involved in photoresponses (e.g., chloroplast photorelocation, phototaxis, stomata reopening) and photomorphogenesis (e.g., shoot and petiole elongation, leaf thickening) (Huché-Thélier et al., 2016; Demotes-Mainard et al., 2016), and it is important to consider how these differences might influence biomass accumulation, yields, and photosynthetic performance in DEPI-grown plants relative to plants grown under natural sunlight. However, new LED lights are becoming available, and we are currently testing a version of the instrument with improved spectral balance using modified LED phosphors and supplemental LED lighting. A second important limitation is that the illumination system provides light at a constant geometry, whereas the angle of sunlight changes throughout the diurnal cycle or is scattered on cloudy days. This difference in light trajectories should influence the distribution of light in complex plants, which is potentially important for light use efficiency. It is also important to note that absorption of light is dependent on leaf angle, and although this effect is minimal in *Arabidopsis*, it should be taken into consideration in crop plants.

The utility of the DEPI technology was demonstrated by detection of, and subsequent high-throughput screening for, complex phenotypes that would otherwise be extremely difficult to characterize. These phenotypes appear under non-laboratory conditions, are highly transient, and are both temporally and spatially heterogeneous and depended in complex ways on the genotype, environment, and developmental stage. The tight control of environmental conditions and simultaneous imaging of all plants enabled DEPI to observe these behaviors reproducibly (Figures 2, 3, and 4) and, thus, to study in detail phenomena relevant to natural or agricultural conditions.

We followed up in some detail on the peculiar patchy phenotypes that appeared in a set of mutants following fluctuating light, partly because this type of phenomenon has not, to our

knowledge, been reported, and also because it allowed us to demonstrate some of the advanced capabilities of the DEPI platform. These effects appeared some time after exposure to high and fluctuating light (Figure 5; Figure S7) so that they would not have normally been observed in photoinhibition experiments. The time delay also suggests that they are not directly caused by the initial photoinhibition processes but could be related to slower repair or remodeling of photosynthesis, which leads to acclimation, as suggested by the fact that these regions appear less sensitive to subsequent fluctuating light treatments (see, for example, leaf-specific phenotypes on days 3 and 5 in Figure 3). Analysis of various chlorophyll fluorescence parameters led us to propose that the effects are related to the formation of a fraction of PSII centers defective in Q_A^- re-oxidation (Figure 6), possibly related to damage to the PSII Q_B site (Chylla and Whitmarsh, 1989) or oxygen-evolving complex, which affects the Q_A redox potential (Krieger and Rutherford, 1997), or to disassembly and reassembly of PSII centers (Nath et al., 2013; Belgio et al., 2012). Nevertheless, further work is required to characterize the molecular mechanisms of these mutants.

The diversity of the T-DNA lines displaying patchy phenotypes (Table S1) suggests the involvement of a range of different processes that possibly act both directly and indirectly. Some of the genes are proposed to function directly in the light reactions of photosynthesis. For example, both Psb33 (SALK_098173) (Fristedt et al., 2015) and PsbR (SALK_114469) (Liu et al., 2009) have been proposed to be involved in PSII stability and repair cycles and become important under conditions where high rates of damage occur. Similarly, NPQ7 is a chloroplast-localized YCF20-like gene involved in nonphotochemical quenching, but its mechanism is not yet understood (Jung and Niyogi, 2010). In contrast, TPT is a transporter in the chloroplast inner envelope (Schneider et al., 2002), and NDF6 (SALK_056498) is a putative membrane protein that has been proposed to be essential for NDH assembly/activity (Ishikawa et al., 2008). Both of these proteins probably affect PSII reactions indirectly, possibly by affecting metabolic status, leading to alterations in redox status or retrograde signals (Rolland et al., 2006; Sharkey et al., 2004). Similarly, the thylakoid ATP/ADP carrier (SALK_119779) (Thuswaldner et al., 2007) or TAAC, which is proposed to supply the lumen with ATP required for the repair cycle, may also influence the stromal ATP/ADP ratio, which, in turn, can modulate ATP synthase activity (Yin et al., 2010). More recent work suggests that TAAC may also function in the chloroplast envelope as a transporter for plastidic phosphoadenosine phosphosulfate (PAPS) and thus may be critical for plastid sulfur metabolism (Gigolashvili et al., 2012).

In conclusion, we demonstrate that DEPI is a useful platform for focusing biochemical, gene expression, and physiological studies and, ultimately, for connecting genome to phenome. Although this work concentrates on light intensity changes, the DEPI platform can readily be extended to reproduce changes in other environmental parameters; e.g., temperature, humidity, soil moisture, and nutrient levels. Therefore, it is possible to systematically alter parameters, individually or in combination, to reveal a range of responses to distinct environmental combinations that mimic those experienced in the field. The DEPI is also highly modular and can easily be expanded to fit even large growth facilities for dynamic phenotyping of larger crop plants as an integral part of new approaches to plant improvement.

EXPERIMENTAL PROCEDURES

Plants and Growth Conditions

Wild-type (Col-0) and T-DNA insertion mutants of *Arabidopsis* were grown at 21°C, 16 hr:8 hr day/night cycle, 100 μmol photons m^{-2} s^{-1}. Three-week-old plants were transferred to imaging chambers and allowed to acclimate for 24 hr to the LED lighting before the start of the experiments. Homozygous seed lines for SALK_098173 (Rieske type Fe-S protein, At1g71500), SAIL_115_E08 (NADPH-dependent thioredoxin reductase, At2g41680), and SALK_103895 (NFU domain protein 3, At4g25910) were obtained from the Chloroplast 2010 Project (Lu et al., 2011).

Design and Construction of DEPI

As illustrated in Figure 1 and Figures S13 and S14, DEPI was designed to control key environmental parameters, including temperature, humidity, and illumination with white (growth) light at intensities and dynamics found in natural environments. DEPI allows sensitive imaging of chlorophyll fluorescence parameters without moving plants or cameras.

DEPI Actinic Lighting

White actinic illumination was provided by 50-W white LED arrays (BXRA-56C5300, Bridgelux) mounted in low-thermal-resistance heat sinks (North American Extrusions, Heat Sink Profile 79000, Aavid Thermalloy) and arranged in 9-cm (center to center) square grids (Figure 1A). The illumination system is scalable to even large matrices. Banks of 48 LEDs (6 × 8) were used in small prototype systems, and tiles of larger banks containing 156 LEDs (6 × 26) were used in the current imaging system assembled inside an environmentally controlled plant growth chamber (Bigfoot FLXC-19 with base dimensions of 0.76 ×2.46 m, BioChambers) modified to accommodate the DEPI lighting, sensors, and control circuits and software. Output light intensity was regulated by a master computer through an I²C serial electronic control bus as described in more detail in Figure S13, a technical schematic showing integration of power and control systems with LED and camera arrays. To minimize edge effects, LED lighting was controlled in 16 individual zones that were calibrated to maintain even illumination. Saturating illumination required for measurement of certain chlorophyll fluorescence parameters was achieved by pulsing the LED arrays for 0.3 s at high current using supplemental lead acid battery power. LEDs were fitted with collimating optics (Britney-M reflector, LEDIL) to increase the intensity at the leaf surface and to better simulate solar irradiance. Illumination intensities were measured using a quantum sensor (LI-COR Biosciences). The current imaging systems can achieve continuous illumination intensities at about 5° dispersion in excess of full sunlight (>2,500 μmol photons m^{-2} s^{-1}) with 0.5-s saturation pulse intensities in excess of 15,000 μmol photons m^{-2} s^{-1} at a distance of 0.5 m from the light sources. Intensities varied by less than 3% across the planting region. For some experiments, far red illumination was supplied by an array of 730-nm LEDs (ELSH-Q61F1-0LPNM-JF3F8, Everlight Electronics).

DEPI Probe Illumination

Light pulses for measuring chlorophyll parameters were provided by a matrix of red-emitting LEDs (Luxeon Rebel SMT High Power LED Red, LXM2-PD01-0050, Philips Lumiled) with collimating optics (FA10993_LISA2-W-PIN-RE, LEDIL; OPC1-2-COL reflector, Dialight). The LEDs were distributed throughout the chamber to achieve even probe illumination (Figure 1A). Probe LEDs were pulsed (10- to 50-μs duration) through a rapid gating circuit (Figure S13) to provide high sensitivity and time resolution but low integrated incident radiation.

DEPI Cameras

Images of chlorophyll fluorescence were captured using high-resolution monochrome CCD cameras with extended near-infrared (nIR) sensitivity (KPV145MC, Hitachi) and fitted with a low-distortion, 8-mm focal length, 2-megapixel C-mount lens (LM8JCM, Kowa Optical Products) and with an optical filter that blocks visible light but passes nIR light (Hoya RT830 or Schott RG9, Edmund Optical). By synchronizing LED pulses and image capture

across multiple arrays, DEPI can image large populations without moving plants or cameras. This feature also allows DEPI to be readily scalable to larger settings. The current version incorporated an array of five cameras in a single chamber.

Image capture was triggered during an ~100-μs dark interval during which actinic or saturating light was electronically shuttered (Figure S14). The measuring pulse occurred 10–35 μs after switching off the actinic light. Systematically varying the timing showed that this delay was sufficiently short to prevent substantial decay of fluorescence properties. The rise in fluorescence induced by a series of measuring pulses in dark-adapted leaves, as described by Kramer et al. (1990), shows that each measuring pulse excited less than 1% of photosystem II centers. This measurement method yields estimates of relative chlorophyll fluorescence yield because pulse-to-pulse intensities, camera gain settings, and optical filter combinations are held constant. Also, by eliminating spectral contamination of chlorophyll fluorescence in the near-infrared by actinic illumination, the method allows measurements under arbitrary light quality actinic illumination, including especially the white light used for growth.

DEPI Controller and Software

Control software was developed in the JAVA language (Netbeans 7.3, http://www.netbeans.org) with supplemental code developed in Visual C++ (Microsoft Visual Studio 2010) using drivers/libraries/SDKs provided by the camera manufacturer. Signals for setting light intensity, gating actinic light, gating the saturation pulse, controlling measuring pulses, and triggering cameras (Figure S13) were generated by a 50-MHz resolution digital programmable timer by programming a field-programmable gate array (FPGA, Nexsys-2, Digilent) using the Verilog language (http://www.verilog.com/).

Image Processing and Analysis

Image capture protocols were patterned to measure standard saturation pulse chlorophyll fluorescence parameters, as reviewed previously (Baker et al., 2007; Baker and Oxborough, 2004). Images were captured before, during, and after the application of saturating actinic illumination. Typically, five frames for each phase (15 frames total) were collected with a 60-ms delay between images. Corrections were applied to account for artifacts caused by residual electrons in the CCD array that occurred during saturating light exposure. These sequences of images were collected before the beginning of each daylight cycle (F_0, F_M, in the absence or presence of saturating actinic light, respectively) as well as immediately before (F_S, F_M', in the absence or presence of saturating actinic light, respectively) and at the end of each 2-min dark period (F_M'', in the presence of saturating actinic light). Image sequences were used to calculate the quantum yield of ϕ_{II}, NPQ, q_E, and q_I, which may reflect photoinhibition (Baker and Oxborough, 2004). This 2-min time was chosen to selectively measure the q_E response. Although q_E has been often been measured after 5–30 min of dark, recent work (Nilkens et al., 2010; Johnson et al., 2008) has shown that relaxation of quenching is separable into several kinetic components. The q_E component is the most rapid, relaxing within the first 2 min, whereas components related to zeaxanthin-dependent processes (q_Z), state transitions (q_T), and movements of chloroplasts (Cazzaniga et al., 2013; Horton and Hague, 1988) and photoinhibition relax in the time ranges from 10 min to several hours. It follows that our q_I estimates may also include contributions from q_Z and other slowly relaxing components, including q_T and movements of chloroplasts (Cazzaniga et al., 2013; Horton and Hague, 1988).

Data analysis was performed using software developed in-house based on the open source software resources ImageJ (http://rsbweb.nih.gov/ij/; Schneider et al., 2012) and Netbeans 7.3 (http://www.netbeans.org) and will be described in detail in a separate publication. The package allows the calculation and visualization of photosynthetic parameters across selected regions of interest and over variable time ranges.

To detect patchy phenotypes, an algorithm was designed to flag mutants in which ϕ_{II} variance was high. Pixels for each plant were binned based on intensity. Absolute range was calculated from the minimum and maximum pixel intensities after exclusion of the upper (highest intensities) and lower (lowest intensities) 2% of the population. Ranges were normalized to the mean intensities to bias the selection for plants where Φ_{II} decreases dramatically. From a pool of candidates exhibiting an average range of ϕ_{II} in excess of ~0.65 (which included 20–30 lines), patchiness was confirmed by visual examination of the images in 12 lines.

SUPPLEMENTAL INFORMATION

Supplemental Information includes fourteen figures, one table, and four movies and can be found with this article online at http://dx.doi.org/10.1016/j.cels.2016.06.001.

AUTHOR CONTRIBUTIONS

DEPI was designed by D.M.K., J.A.C., R.Z., C.C.H., and K.K. Control software for the DEPI was developed by C.C.H., K.K., and J.A.C. The high-throughput REP screening experiment was designed by L.J.S., J.A.C., and D.M.K. L.J.S. managed the execution of this experiment. Other experiments were designed and performed by J.A.C., M.S.C., and G.A.D. Software tools for image processing were developed by J.C., J.A.C., and C.C.H. Software tools for data analysis were developed by J.C. with input from D.M.K., L.J.S., and J.A.C. Data analysis was performed by J.A.C., L.J.S., M.S.C., G.A.D., J.C., and D.M.K. The manuscript was written primarily by J.A.C., D.M.K., and L.J.S.

REFERENCES

Ajjawi, I., Lu, Y., Savage, L.J., Bell, S.M., and Last, R.L. (2010). Large-scale reverse genetics in Arabidopsis: case studies from the Chloroplast 2010 Project. Plant Physiol. 152, 529–540.

Attaran, E., Major, I.T., Cruz, J.A., Rosa, B.A., Koo, A.J., Chen, J., Kramer, D.M., He, S.Y., and Howe, G.A. (2014). Temporal Dynamics of Growth and Photosynthesis Suppression in Response to Jasmonate Signaling. Plant Physiol. 165, 1302–1314.

Baker, N.R., and Oxborough, K. (2004). Chlorophyll fluorescence as a probe of photosynthetic productivity. In Chlorophyll a Fluorescence: A Signature of Photosynthesis, G.C. Papageorgiou and Govindjee., eds. (Springer), pp. 65–82.

Baker, N.R., Oxborough, K., Lawson, T., and Morison, J.I.L. (2001). High resolution imaging of photosynthetic activities of tissues, cells and chloroplasts in leaves. J. Exp. Bot. 52, 615–621.

Baker, N.R., Harbinson, J., and Kramer, D.M. (2007). Determining the limitations and regulation of photosynthetic energy transduction in leaves. Plant Cell Environ. 30, 1107–1125.

Belgio, E., Johnson, M.P., Jurić, S., and Ruban, A.V. (2012). Higher plant photosystem II light-harvesting antenna, not the reaction center, determines the excited-state lifetime-both the maximum and the nonphotochemically quenched. Biophys. J. 102, 2761–2771.

Blankenship, R.E., Tiede, D.M., Barber, J., Brudvig, G.W., Fleming, G., Ghirardi, M., Gunner, M.R., Junge, W., Kramer, D.M., Melis, A., et al. (2011). Comparing photosynthetic and photovoltaic efficiencies and recognizing the potential for improvement. Science 332, 805–809.

Boyer, J.S. (1982). Plant productivity and environment. Science 218, 443–448.

Braam, J. (2005). In touch: plant responses to mechanical stimuli. New Phytol. 165, 373–389.

Braam, J., and Davis, R.W. (1990). Rain-, wind-, and touch-induced expression of calmodulin and calmodulin-related genes in Arabidopsis. Cell 60, 357–364.

Bresson, J., Vasseur, F., Dauzat, M., Koch, G., Granier, C., and Vile, D. (2015). Quantifying spatial heterogeneity of chlorophyll fluorescence during plant growth and in response to water stress. Plant Methods 11, 23.

Cazzaniga, S., Dall' Osto, L., Kong, S.-G., Wada, M., and Bassi, R. (2013). Interaction between avoidance of photon absorption, excess energy

dissipation and zeaxanthin synthesis against photooxidative stress in Arabidopsis. Plant J. *76*, 568–579.

Chylla, R.A., and Whitmarsh, J. (1989). Inactive Photosystem II Complexes in Leaves : Turnover Rate and Quantitation. Plant Physiol. *90*, 765–772.

Chylla, R.A., Garab, G., and Whitmarsh, J. (1987). Evidence for slow turnover in a fraction of Photosystem II complexes in thylakoid membranes. Biochim. Biophys. Acta *894*, 562–571.

Demotes-Mainard, S., Péron, T., Corot, A., Bertheloot, J., Le Gourrierec, J., Pelleschi-Travier, S., Crespel, L., Morel, P., Huché-Thélier, L., Boumaza, R., et al. (2016). Plant responses to red and far-red lights, applications in horticulture. Environ. Exp. Bot. *121*, 4–21.

Dutta, S., Cruz, J.A., Jiao, Y., Chen, J., Kramer, D.M., and Osteryoung, K.W. (2015). Non-invasive, whole-plant imaging of chloroplast movement and chlorophyll fluorescence reveals photosynthetic phenotypes independent of chloroplast photorelocation defects in chloroplast division mutants. Plant J. *84*, 428–442.

Friso, G., Giacomelli, L., Ytterberg, A.J., Peltier, J.B., Rudella, A., Sun, Q., and Wijk, K.J. (2004). In-depth analysis of the thylakoid membrane proteome of Arabidopsis thaliana chloroplasts: new proteins, new functions, and a plastid proteome database. Plant Cell *16*, 478–499.

Fristedt, R., Herdean, A., Blaby-Haas, C.E., Mamedov, F., Merchant, S.S., Last, R.L., and Lundin, B. (2015). PHOTOSYSTEM II PROTEIN33, a protein conserved in the plastid lineage, is associated with the chloroplast thylakoid membrane and provides stability to photosystem II supercomplexes in Arabidopsis. Plant Physiol. *167*, 481–492.

Gaspar, T., Franck, T., Bisbis, B., Kevers, C., Jouve, L., Hausman, J.F., and Dommes, J. (2002). Concepts in plant stress physiology. Application to plant tissue cultures. Plant Growth Regul. *37*, 263–285.

Gigolashvili, T., Geier, M., Ashykhmina, N., Frerigmann, H., Wulfert, S., Krueger, S., Mugford, S.G., Kopriva, S., Haferkamp, I., and Flügge, U.-I. (2012). The Arabidopsis thylakoid ADP/ATP carrier TAAC has an additional role in supplying plastidic phosphoadenosine 5′-phosphosulfate to the cytosol. Plant Cell *24*, 4187–4204.

Grieco, M., Tikkanen, M., Paakkarinen, V., Kangasjärvi, S., and Aro, E.M. (2012). Steady-state phosphorylation of light-harvesting complex II proteins preserves photosystem I under fluctuating white light. Plant Physiol. *160*, 1896–1910.

Horton, P., and Hague, A. (1988). Studies on the induction of chlorophyll fluorescence in isolated barley protoplasts. IV. Resolution of non-photochemical quenching. Biochim. Biophys. Acta *932*, 107–115.

Huché-Thélier, L., Crespel, L., Gourrierec, J.L., Morel, P., Sakr, S., and Leduc, N. (2016). Light signaling and plant responses to blue and UV radiations—Perspectives for applications in horticulture. Environ. Exp. Bot. *121*, 22–38.

Ishikawa, N., Takabayashi, A., Ishida, S., Hano, Y., Endo, T., and Sato, F. (2008). NDF6: a thylakoid protein specific to terrestrial plants is essential for activity of chloroplastic NAD(P)H dehydrogenase in Arabidopsis. Plant Cell Physiol. *49*, 1066–1073.

Johnson, M.P., Davison, P.A., Ruban, A.V., and Horton, P. (2008). The xanthophyll cycle pool size controls the kinetics of non-photochemical quenching in Arabidopsis thaliana. FEBS Lett. *582*, 262–266.

Jung, H.-S., and Niyogi, K.K. (2010). Mutations in Arabidopsis YCF20-like genes affect thermal dissipation of excess absorbed light energy. Planta *231*, 923–937.

Kanazawa, A., and Kramer, D.M. (2002). In vivo modulation of nonphotochemical exciton quenching (NPQ) by regulation of the chloroplast ATP synthase. Proc. Natl. Acad. Sci. USA *99*, 12789–12794.

Kohzuma, K., Dal Bosco, C., Kanazawa, A., Dhingra, A., Nitschke, W., Meurer, J., and Kramer, D.M. (2012). Thioredoxin-insensitive plastid ATP synthase that performs moonlighting functions. Proc. Natl. Acad. Sci. USA *109*, 3293–3298.

Kramer, D.M., and Crofts, A.R. (1996). Control of photosynthesis and measurement of photosynthetic reactions in intact plants. In Photosynthesis and the environment, N.R. Baker, ed. (Dordrecht, The Netherlands: Kluwer Academic Press).

Kramer, D.M., and Evans, J.R. (2011). The importance of energy balance in improving photosynthetic productivity. Plant Physiol. *155*, 70–78.

Kramer, D.M., Robinson, H.R., and Crofts, A.R. (1990). A portable multi-flash kinetic fluorimeter for measurement of donor and acceptor reactions of Photosystem 2 in leaves of intact plants under field conditions. Photosynth. Res. *26*, 181–193.

Krieger, A., and Rutherford, A.W. (1997). Comparison of chloride-depleted and calcium-depleted PSII: the midpoint potential of QA and susceptibility to photodamage. Biochim. Biophys. Acta *1319*, 91–98.

Külheim, C., Agren, J., and Jansson, S. (2002). Rapid regulation of light harvesting and plant fitness in the field. Science *297*, 91–93.

Lawson, T., Weyers, J., and A'Brook, R. (1998). The nature of heterogeneity in the stomatal behaviour of Phaseolus vulgaris L. primary leaves. J. Exp. Bot. *49*, 1387–1395.

Liu, H., Frankel, L.K., and Bricker, T.M. (2009). Characterization and complementation of a psbR mutant in Arabidopsis thaliana. Arch. Biochem. Biophys. *489*, 34–40.

Long, S.P., and Bernacchi, C.J. (2003). Gas exchange measurements, what can they tell us about the underlying limitations to photosynthesis? Procedures and sources of error. J. Exp. Bot. *54*, 2393–2401.

Loreto, F., and Sharkey, T.D. (1990). Low humidity can cause uneven photosynthesis in olive (Olea europea L.) leaves. Tree Physiol. *6*, 409–415.

Lu, Y., Savage, L.J., Larson, M.D., Wilkerson, C.G., and Last, R.L. (2011). Chloroplast 2010: a database for large-scale phenotypic screening of Arabidopsis mutants. Plant Physiol. *155*, 1589–1600.

Mishra, Y., Jänkänpää, H.J., Kiss, A.Z., Funk, C., Schröder, W.P., and Jansson, S. (2012). Arabidopsis plants grown in the field and climate chambers significantly differ in leaf morphology and photosystem components. BMC Plant Biol. *12*, 6.

Morgan, D.C., and Smith, H. (1981). Control of development in Chenopodium Album L. by shadelight: The effect of light quantity (total fluence rate) and light quality (red.far-red ratio). New Phytol. *88*, 239–248.

Mott, K.A., and Buckley, T.N. (1998). Stomatal heterogeneity. J. Exp. Bot. *49*, 407–417.

Müller, P., Li, X.P., and Niyogi, K.K. (2001). Non-photochemical quenching. A response to excess light energy. Plant Physiol. *125*, 1558–1566.

Munns, R., James, R.A., Sirault, X.R.R., Furbank, R.T., and Jones, H.G. (2010). New phenotyping methods for screening wheat and barley for beneficial responses to water deficit. J. Exp. Bot. *61*, 3499–3507.

Murchie, E.H., and Niyogi, K.K. (2011). Manipulation of photoprotection to improve plant photosynthesis. Plant Physiol. *155*, 86–92.

Nath, K., Jajoo, A., Poudyal, R.S., Timilsina, R., Park, Y.S., Aro, E.-M., Nam, H.G., and Lee, C.H. (2013). Towards a critical understanding of the photosystem II repair mechanism and its regulation during stress conditions. FEBS Lett. *587*, 3372–3381.

Nedbal, L., and Whitmarsh, J. (2004). Chlorophyll Fluorescence Imaging of Leaves and Fruits. In Chlorophyll a Fluorescence: A Signature of Photosynthesis, C. Papageorgiou and Govindjee., eds. (Kluwer Academic Publishers), pp. 389–407.

Nilkens, M., Kress, E., Lambrev, P., Miloslavina, Y., Müller, M., Holzwarth, A.R., and Jahns, P. (2010). Identification of a slowly inducible zeaxanthin-dependent component of non-photochemical quenching of chlorophyll fluorescence generated under steady-state conditions in Arabidopsis. Biochim. Biophys. Acta *1797*, 466–475.

Omasa, K., Hosoi, F., and Konishi, A. (2007). 3D lidar imaging for detecting and understanding plant responses and canopy structure. J. Exp. Bot. *58*, 881–898.

Oxborough, K. (2004a). Imaging of chlorophyll a fluorescence: theoretical and practical aspects of an emerging technique for the monitoring of photosynthetic performance. J. Exp. Bot. *55*, 1195–1205.

Oxborough, K. (2004b). Using Chlorophyll a Fluorescence Imaging to Monitor Photosynthetic Performance. In Chlorophyll a Fluorescence: A Signature of Photosynthesis, G. Papageorgiou and Govindjee., eds. (Springer), pp. 109–428.

Paproki, A., Sirault, X., Berry, S., Furbank, R., and Fripp, J. (2012). A novel mesh processing based technique for 3D plant analysis. BMC Plant Biol. *12*, 63.

Peltier, J.B., Ytterberg, A.J., Sun, Q., and van Wijk, K.J. (2004). New functions of the thylakoid membrane proteome of Arabidopsis thaliana revealed by a simple, fast, and versatile fractionation strategy. J. Biol. Chem. *279*, 49367–49383.

Poorter, H., Niklas, K.J., Reich, P.B., Oleksyn, J., Poot, P., and Mommer, L. (2012). Biomass allocation to leaves, stems and roots: meta-analyses of inter-specific variation and environmental control. New Phytol. *193*, 30–50.

Rascher, U., and Nedbal, L. (2006). Dynamics of photosynthesis in fluctuating light. Curr. Opin. Plant Biol. *9*, 671–678.

Raven, J.A. (2011). The cost of photoinhibition. Physiol. Plant. *142*, 87–104.

Rolland, F., Baena-Gonzalez, E., and Sheen, J. (2006). Sugar sensing and signaling in plants: conserved and novel mechanisms. Annu. Rev. Plant Biol. *57*, 675–709.

Roy, S.J., Tucker, E.J., and Tester, M. (2011). Genetic analysis of abiotic stress tolerance in crops. Curr. Opin. Plant Biol. *14*, 232–239.

Schäufele, R., Santrucek, J., and Schnyder, H. (2011). Dynamic changes of canopy-scale mesophyll conductance to CO_2 diffusion of sunflower as affected by CO_2 concentration and abscisic acid. Plant Cell Environ. *34*, 127–136.

Schneider, A., Häusler, R.E., Kolukisaoglu, U., Kunze, R., van der Graaff, E., Schwacke, R., Catoni, E., Desimone, M., and Flügge, U.I. (2002). An Arabidopsis thaliana knock-out mutant of the chloroplast triose phosphate/phosphate translocator is severely compromised only when starch synthesis, but not starch mobilisation is abolished. Plant J. *32*, 685–699.

Schneider, C.A., Rasband, W.S., and Eliceiri, K.W. (2012). NIH Image to ImageJ: 25 years of image analysis. Nat. Methods *9*, 671–675.

Sharkey, T.D., Laporte, M., Lu, Y., Weise, S., and Weber, A.P.M. (2004). Engineering plants for elevated CO(2): a relationship between starch degradation and sugar sensing. Plant Biol (Stuttg) *6*, 280–288.

Shur, M.S., and Zukauskas, R. (2005). Solid-State Lighting: Toward Superior Illumination. Proc. IEEE *93*, 1691–1703.

Singsaas, E.L., and Sharkey, T.D. (1998). The regulation of isoprene emission responses to rapid leaf temperature fluctuations. Plant Cell Environ. *21*, 1181–1188.

Sirault, X.R.R., James, R.A., and Furbank, R.T. (2009). A new screening method for osmotic component of salinity tolerance in cereals using infrared thermography. Funct. Plant Biol. *36*, 970–977.

Strand, D.D., Livingston, A.K., Satoh-Cruz, M., Froehlich, J.E., Maurino, V.G., and Kramer, D.M. (2015). Activation of cyclic electron flow by hydrogen peroxide in vivo. Proc. Natl. Acad. Sci. USA *112*, 5539–5544.

Stroppiana, D., Boschetti, M., Brivio, P.A., and Bocchi, S. (2009). Plant nitrogen concentration in paddy rice from field canopy hyperspectral radiometry. Field Crops Res. *111*, 119–129.

Suorsa, M., Järvi, S., Grieco, M., Nurmi, M., Pietrzykowska, M., Rantala, M., Kangasjärvi, S., Paakkarinen, V., Tikkanen, M., Jansson, S., and Aro, E.M. (2012). PROTON GRADIENT REGULATION5 is essential for proper acclimation of Arabidopsis photosystem I to naturally and artificially fluctuating light conditions. Plant Cell *24*, 2934–2948.

Takizawa, K., Cruz, J.A., Kanazawa, A., and Kramer, D.M. (2007). The thylakoid proton motive force in vivo. Quantitative, non-invasive probes, energetics, and regulatory consequences of light-induced pmf. Biochim. Biophys. Acta *1767*, 1233–1244.

Thuswaldner, S., Lagerstedt, J.O., Rojas-Stütz, M., Bouhidel, K., Der, C., Leborgne-Castel, N., Mishra, A., Marty, F., Schoefs, B., Adamska, I., et al. (2007). Identification, expression, and functional analyses of a thylakoid ATP/ADP carrier from Arabidopsis. J. Biol. Chem. *282*, 8848–8859.

Tikkanen, M., Grieco, M., Nurmi, M., Rantala, M., Suorsa, M., and Aro, E.-M. (2012). Regulation of the photosynthetic apparatus under fluctuating growth light. Philos. Trans. R. Soc. Lond. B Biol. Sci. *367*, 3486–3493.

Vadez, V., Berger, J.D., Warkentin, T., Asseng, S., Ratnakumar, P., Rao, K.P.C., Gaur, P.M., Munier-Jolain, N., Larmure, A., Voisin, A.S., et al. (2012). Adaptation of grain legumes to climate change: a review. Agron. Sustain. Dev. *32*, 31–44.

White, J.W., Andrade-Sanchez, P., Gore, M.A., Bronson, K.F., Coffelt, T.A., Conley, M.M., Feldmann, K.A., French, A.N., Heun, J.T., Hunsaker, D.J., et al. (2012). Field-based phenomics for plant genetics research. Field Crops Res. *133*, 101–112.

Yin, L., Lundin, B., Bertrand, M., Nurmi, M., Solymosi, K., Kangasjärvi, S., Aro, E.-M., Schoefs, B., and Spetea, C. (2010). Role of thylakoid ATP/ADP carrier in photoinhibition and photoprotection of photosystem II in Arabidopsis. Plant Physiol. *153*, 666–677.

Zhu, X.G., Long, S.P., and Ort, D.R. (2010). Improving photosynthetic efficiency for greater yield. Annu. Rev. Plant Biol. *61*, 235–261.